Natural Resources for Human Health
eISSN: 2583-1194

Original Research

Received 21 May 2026
Revised 30 June 2026
Accepted 23 July 2026

Natural Resources for Human Health 2026, Vol. 6(10s): 1372–1392

KEYWORDS:
ciclopirox olamine, microneedles, nanogel, onychomycosis, spanlastics, transungual delivery.

Development, Optimisation, and Evaluation of a Ciclopirox Olamine-Loaded Spanlastic Nanogel with Microneedle Pen Pre-Treatment for Enhanced Transungual Drug Delivery

Salah Ali Shakir[1]*, Mohammed Hussain Al-Mayahy[1]

[1]Department of Pharmaceutics, College of Pharmacy, Mustansiriyah University, Baghdad, Iraq
*salah1995@uomustansiriyah.edu.iq

ABSTRACT:

Background: Onychomycosis is a chronic fungal infection of the nails that is difficult to treat in which the dense keratinised nail plate restricts drug permeation.

Objective: To develop, optimise ciclopirox olamine (CPO) loaded spanlastic (SP) nanogel formulations and investigate the potential of microneedle (MN) pre-treatment to enhance CPO permeation into the nail as a topical approach for the treatment of onychomycosis.

Methods: The formulations were designed and optimised using a Box–Behnken experimental design. SPs were prepared using different concentrations of Span 60 and Tween 80. The optimised SP formulation was characterised and subsequently incorporated into Carbopol 934P gel bases to prepare SP nanogels, which were evaluated to select the optimum formulation. *Ex vivo* permeation studies using sheep hooves and human fingernails were conducted to determine the amounts of CPO permeated through and deposited within the nail from the optimum SP nanogel, with and without MN pre-treatment.

Results: The optimised SP formulation exhibited an appropriate vesicle size, PDI, and entrapment efficiency, with enhanced antifungal activity. The optimum SP nanogel showed suitable vesicle size, PDI, viscosity, drug content, and drug release characteristics. The ex vivo permeation study demonstrated greater CPO deposition from the SP nanogel than from the plain gel, with 1.54-fold and 1.73-fold increases in deposition in sheep hooves and human fingernails, respectively. Furthermore, MN pen pre-treatment markedly enhanced CPO deposition, resulting in 76% and 55% increases in sheep hooves and human fingernails, respectively, compared with the corresponding formulations without MN pre-treatment.

Conclusion: The combination of SP nanogel formulation with MNs represents a promising strategy for enhancing transungual drug delivery for the topical treatment of onychomycosis.

1. INTRODUCTION

The human nail is the largest and most complicated skin appendage. It is a unique keratinous structure that is important for protection and feeling [1]. The nail plate, which is the main barrier, has different layers that make it firm, flexible, and stick to the nail bed [2-4]. This dense structure is composed of sulphur matrix proteins and strong keratins, which make it very difficult to penetrate. Onychomycosis is the predominant nail infection globally; it alters the hue of the nail plate, increases its thickness, and leads to its deterioration [5, 6]. Previously thought to be caused by dermatophytes, new research shows that non-

dermatophyte moulds and mixed infections play a major role, especially in warmer areas [6]. Distal subungual onychomycosis is the most prevalent clinical manifestation, distinguished by onycholysis, subungual hyperkeratosis, and discolouration [4, 7, 8].

The problems associated with systemic treatment, such as oral terbinafine, itraconazole, and fluconazole, are significant. Systemic therapy is constrained by elevated dosages, extended treatment durations, considerable adverse effects, medication interactions, and contraindications [9, 10]. While the topical therapy is severely hindered by the formidable barrier properties of the nail plate. Drug permeation is critically limited by molecular size, lipophilicity, vehicle pH, and hydration state [11]. Chemical enhancers such as urea, thioglycolic acid, and keratolytics can break up keratin bonds and make the skin more hydrated [12, 13]. Physical methods such as abrasion, microneedling, and avulsion can also break down this barrier [14, 15]. However, it is still challenging to obtain therapeutic concentrations at the site of infection. Ciclopirox olamine (CPO) is a hydroxypyridone derivative available worldwide in several formulations for the treatment of superficial fungal and yeast infections, vaginal candidiasis, seborrhoeic dermatitis, and onychomycosis. It demonstrates improved properties in its affinity for keratin and its capacity to penetrate nails. It has shown superior efficacy and safety relative to another commercially available formulation in the treatment of onychomycosis [16].

CPO has exhibited both fungicidal and fungistatic properties towards various pathogenic organisms, including dermatophytes such as Trichophyton, Microsporum, and Epidermophyton genera [17]. The antifungal effectiveness of CPO can be attributed to the modification of cell permeability and to its ability to chelate intracellular metals, such as iron

[16, 18]. CPO is currently available in many formulations, such as creams, gels, suspensions, solutions, lotions, nail lacquers, and shampoos [19, 20].

Nanocarriers represent an advanced approach to passing across the nail barrier. One of these technologies is spanlastics (SPs), which are highly flexible vesicles based on non-ionic surfactants and edge activators, signifying a notable breakthrough [21-23]. These elastic vesicles work as a drug delivery system, which moves through spaces between cells and through biological membranes. The distinctive structure of SPs, arising from less interfacial tension and bilayer breakdown, imparts enhanced deformability relative to liposomes or niosomes [24]. SPs exhibit increased permeability, enhanced stability, reduced cost, and variety in administration routes, including topical and transungual delivery [22, 24-26]. Thus, the aim of this study was to develop, optimise a CPO-loaded SP nanogel and investigate its ability to enhance drug permeation and deposition within the nail plate, with and without MN pre-treatment. This approach may provide a promising platform for overcoming the highly restrictive nail barrier and improving topical antifungal drug delivery for the treatment of onychomycosis.

2. MATERIALS AND METHODS

2.1. Materials

CPO was purchased from Bide Pharma, China. Span 60 and Tween 80 were ordered from Thomas Baker Chemicals, India. All other chemicals and solvents were of analytical grade.

2.2. Experimental Design

Design-Expert® version 13 (Stat-Ease, Inc. USA) was used to generate and analyse the experimental design for formulation optimisation. The Box-Behnken model, a response surface methodology (RSM) design, was selected because of its efficiency and the requirement of fewer experimental runs than other models. As shown in Table 1, this model was used to evaluate the effects of independent variables, specifically (X1) surfactant "Span 60" concentration, (X2) edge activator concentration "Tween 80", and (X3) sonication time and their combination on three responses. The measured responses include (Y1) vesicle size (VS), (Y2) polydispersity index (PDI), and (Y3) entrapment efficiency (EE%). Each independent variable was investigated at three coded levels (+1, 0, -1), corresponding to the low, centre, and high levels, respectively. For three independent variables, the Box-Behnken design generated 15 experimental runs, consisting of 12 edge points and three replicated centre points to estimate the pure experimental error and evaluate model adequacy. Accordingly, the experimental design consisted of 15 formulation runs, as presented in Table 2.

Table 1. Independent variables and responses used in Box-Behnken design for the formulation trials.

Factors (Independent variables)	**Levels**		
	(High)	**(Medium)**	**(Low)**
	+1	**0**	**-1**
X1: Conc. of surfactant: Span 60 (mg/mL)	60	40	20
X2: Conc. of edge activator: Tween 80 (mg/mL)	40	25	10
X3: Sonication time (min.)	5	2.5	0
Responses (Dependent variables)	**Desirability constraints**		
Y1: Vesicle size (VS) (nm)	Minimize		
Y2: Polydispersity index (PDI)	Minimize		
Y3: Entrapment efficiency (EE%)	Maximize		

2.3. Preparation of ciclopirox olamine spanlastics

The ethanol injection method was used to prepare SPs formulations. This method is extensively used to prepare SPs since it is simple, cheap, and convenient [27]. First, to prepare the aqueous phase, the required amount of Tween 80 for each formula was placed in a 25 mL beaker, and then 10 mL of deionised water was added. After that, the water phase was placed on a magnetic stirrer that was set to 65°C and stirring at 1000 rpm. The organic phase was prepared by dissolving CPO and the required amount of Span 60 for each formula in 5 mL of ethanol [28]. Subsequently, the organic phase was injected dropwise into the hot aqueous phase and stirred on a magnetic stirrer at 1000 rpm for 30 minutes. After that, the mixture was sonicated for the specified duration as per the preparation design. Finally, the product was transferred to sealed glass vials for storage at 4°C until further characterisation [21].

2.4. Characterisation of the prepared ciclopirox olamine spanlastics

2.4.1. Measurement of vesicle size and polydispersity index

Measurements of the vesicle size and PDI have been performed with the Litesizer DLS 500 instrument (Anton Paar, Austria) through the dynamic light scattering (DLS) technique. The samples were diluted with deionised water in two steps at a ratio of 1:1000 and mixed by vortex mixer for 1 minute to ensure uniform dispersion. The measurement was conducted at a temperature of 20°C [28].

2.4.2. Entrapment efficiency determination

The entrapment efficiency was determined using a cooling centrifuge (Hermle Z216 MK Benchmark, USA). One millilitre of the SPs formulation was transferred to a centrifuge tube to be centrifuged at 15,000 rpm for an hour at 4°C. Upon completion of the designated time, the supernatant containing the unentrapped (free) CPO was collected and the concentration of free drug was determined by measuring the absorbance at 306 nm utilising a UV-visible spectrophotometer (Shimadzu UV-1900i Plus, Japan). This procedure was done in triplicate [29]. The entrapment efficiency was determined using equation 1:

EE% = (Total amount of CPO - Amount of free CPO) ×100/Total amount of CPO **……Eq. (1)**

2.4.3. Zeta potential determination

The zeta potential of the optimised SPs formulation was determined to evaluate its surface charge and predict the stability. The measurement was performed using a Litesizer DLS 500 zeta potential analyser (Anton Paar, Austria). The sample being examined was diluted with deionised water and then transferred into a zeta potential cuvette. The measurement was done in triplicate, and the results were expressed as a mean ± SD [30].

2.4.4. Transmission Electron Microscopy

Transmission electron microscopy (TEM) was performed to examine the morphology and vesicular structure of the optimised CPO SPs formulation using a JEM-1010 transmission electron microscope (JEOL Ltd., Japan). A small aliquot of the formulation was placed onto a carbon-coated copper grid and allowed to adsorb. The excess sample was carefully removed using filter paper, and the grid was negatively stained with 2% (w/v) uranyl acetate for 30 minutes to enhance image contrast. After air-drying, the samples were examined at an accelerating voltage of 120 kV and a magnification of 50,000X [30].

2.4.5. *In vitro* antifungal activity study

Using the agar well diffusion method, the antifungal activity of pure CPO and the optimised SPs formulation was assessed against Trichophyton spp. On Sabourated Dextrose Agar (SDA) plates, Trichophyton spp. were cultured at 28°C for 7–10 days to obtain sufficient fungal growth. The fungal colonies were harvested and suspended in sterile distilled water to prepare the inoculum. The prepared inoculum was uniformly spread over the surface of freshly prepared SDA plates using a sterile cotton swab. Using a sterile cork borer, holes were made in the centre of the agar. After that, CPO was dissolved in DMSO to prepare a pure CPO culture solution. Three groups were evaluated: (i) pure CPO solution, (ii) blank SPs formulation (containing the formulation components without CPO), and (iii) CPO-loaded SPs formulation. Fifty microliters (50 µL) of each sample were carefully introduced into the respective wells. The plates were subsequently incubated at 28°C for 72 hours. Following incubation, the antifungal activity was assessed by measuring the diameter of the inhibition zone surrounding each well using a ruler, and the results were expressed in millimetres. All experiments were performed in triplicate, and the mean inhibition zone diameter was calculated [31].

2.5. Preparation of spanlastic nanogel and plain gel

The SP nanogel was formulated by mixing the SP solution with Carbopol 934P gel base. First, Carbopol 934P was dispersed gently in deionised water with constant stirring of 120 rpm for 3 hours at 25°C using a magnetic stirrer (Dragon Lab, USA). In order to adjust the pH of the gel formulation to 7, triethanolamine was added dropwise to the gel base, and the mixture was stirred at 100 rpm. The gel was then allowed to stand overnight to remove the entrapped air and ensure complete hydration and neutralization of Carbopol 934P. After that, the SP solution of CPO was added to the gel base at a ratio of 1:1 with stirring at 1000 rpm to obtain a homogeneous dispersion [32]. To investigate the influence of the gelling agent concentration, four concentrations of the Carbopol 934P (0.25, 0.5, 0.75, 1% w/w) were used to prepare the SP nanogels SPNG1, SPNG2, SPNG3, and SPNG4, respectively. A plain gel of CPO was prepared using the same procedure for the preparation of SP nanogels. The only difference was the use of CPO solution instead of SP of CPO when mixed with the gel base.

2.6. Characterisation of the prepared spanlastics nanogel

2.6.1. Viscosity measurement

The viscosity and rheological behaviour of the prepared SP nanogel formulations were evaluated using a Brookfield DV-E rotational viscometer (Brookfield LVDVE, USA). Measurements were performed using spindle No. 64 at 25 ± 0.5°C. The rotational speed was initially set at 10 rpm and then gradually increased to 100 rpm to evaluate the effect of shear on the gel viscosity. The viscosity values were recorded at each rotational speed. All measurements were performed in triplicate, and the results were expressed as mean ± SD [29].

2.6.2. Determination of drug content

The drug content of the optimised SP nanogel formulation was determined by UV-visible spectrophotometry. Briefly, 1 g of the nanogel was accurately weighed and dissolved in 100 mL of ethanol under continuous stirring to ensure complete extraction of CPO. The resulting solution was filtered and its absorbance was measured at 306 nm using a UV-visible spectrophotometer (Shimadzu UV-1900i Plus, Japan). All measurements were performed in triplicate, and the results were expressed as mean ± SD [29].

2.6.3. *In vitro* release study

The *in vitro* release study was performed using Franz cell diffusion apparatus with a surface area of 0.785 cm^2. A cellulose nitrate membrane with pores of 0.45 µm was utilised as a release membrane. The donor compartment of the Franz cell was loaded with 1 g of each SP nanogel formulations SPNG1, SPNG2, SPNG3, and SPNG4. The receptor compartment was filled with

10 mL of PBS pH 7.4, which was stirred by a Teflon-coated magnetic bar at 100 rpm and maintained at a temperature of 37 ± 0.5°C throughout the experiment. Samples of 0.5 mL were withdrawn from the receptor compartment at pre-arranged intervals of 0.5, 1, 2, 4, 8, and 12 hours. The withdrawn samples were immediately replaced with an equal volume of fresh prewarmed PBS maintained at the same temperature to preserve sink conditions and a constant receptor volume. The concentration of CPO released was determined using a UV-visible spectrophotometer (Shimadzu UV-1900i Plus, Japan) at 306 nm. The cumulative percentage of drug released was plotted as a function of time. All experiments were performed in triplicate, and the results were expressed as mean ± SD [33].

2.6.4. Measurement of vesicle size, polydispersity index, and zeta potential

The vesicle size and PDI of the optimised SP nanogel formulation were determined according to the method described in Section 2.4.1, following appropriate dilution of the nanogel with deionised water. Similarly, the zeta potential of the optimised nanogel formulation was measured to evaluate the surface charge and colloidal stability of the incorporated SPs vesicles, as described in Section 2.4.3.

2.6.5. Field emission Scanning Electron Microscopy (Fe-SEM)

The surface morphology of the optimised SP nanogel formulation was examined using a field emission scanning electron microscope (FE-SEM; FEI Company, USA). A small amount of the nanogel was spread onto an aluminium specimen stub and allowed to dry completely. The dried sample was then sputter-coated with a thin layer of gold to improve its electrical conductivity prior to imaging. The micrographs were captured at appropriate magnifications to evaluate the surface morphology and distribution of the incorporated SP vesicles [34].

2.6.6. *Ex vivo* permeation study

The *ex vivo* permeation of CPO from the optimised SP nanogel and the plain gel was conducted through sheep hooves and human fingernails using Franz diffusion cell apparatus. Human nails samples were obtained from 25–35-year male volunteers, while sheep hooves samples were collected from one year old sheep. The volunteers signed a consent form to collect and use their fingernails in laboratory work. The hooves and nails were cleaned carefully and cut into small pieces at a size approximately corresponding to the surface area of the Franz cells of 0.785 cm^2. The nails (n = 6) were mounted between the donor and receptor compartments and fixed using a silicon adhesive. After that, the nail surface was cleaned again to remove any adhesive residue from the fixation process. The receptor compartment was filled with PBS pH 7.4, while the donor compartment was loaded with 1 g of the formulations equivalent to 1% of CPO. The receptor fluid was maintained at 37 ± 0.5°C and continuously stirred at 100 rpm using a magnetic stirrer. Samples of 0.5 mL were withdrawn from the receptor fluid at predetermined time intervals (1, 2, 4, 8, 12, and 24 hours) and immediately replaced with an equal volume of fresh prewarmed PBS to maintain a constant receptor volume and sink conditions. After that, the samples were measured at 306 nm by a UV-visible spectrophotometer to calculate the cumulative permeated amount of CPO.

Following completion of the permeation study, the hooves and nails were removed from the Franz cells to determine the amount of CPO retained within the tissues. Each specimen was cut into small pieces and immersed in 10 mL of PBS (pH 7.4) for 24 hours, followed by sonication in an ultrasonic bath (Elma, Germany) for an hour to facilitate drug extraction. The extracted samples were subsequently analysed using the UV-visible spectrophotometer at 306 nm, and the CPO amount retained was quantified.

2.6.7. Pre-treatment with microneedle pen device

To assess the impact of microneedling technique on the permeation of CPO from the SP nanogel and plain gel, hooves and nail pieces (n = 6) were cleaned and hydrated by immersion in PBS pH 7.4 for 24 hours [35]. After that, they were gently blotted dry and positioned on a flat rigid surface. Nail microporation was then performed by vertically applying a MN pen equipped with 12 stainless-steel MNs in one pass for one minute [36]. The device was operated at a needle length of 1 mm with a minimum vibration speed of 4000 oscillation per minute. Subsequently, the samples were mounted onto the Franz cells, and the *ex vivo* permeation study was performed under the same experimental conditions described previously in Section 2.6.6 [37].

2.6.8. Stability study of spanlastic nanogel

The stability of the optimised SP nanogel formulation was evaluated over a period of 3 months. The formulation was stored in tightly closed glass vials at 4°C, 25°C, and 40°C. At a regular monthly interval, the samples were withdrawn and tested for pH,

vesicle size, PDI, and drug content using the methods described previously. All measurements were performed in triplicate, and the results were expressed as mean ± SD.

3. RESULTS AND DISCUSSION

3.1. Characterisation of ciclopirox olamine spanlastics

3.1.1. Measurement of the vesicle size, polydispersity index and entrapment efficiency

The results for vesicle size (VS), polydispersity index (PDI), and entrapment efficiency (EE%) of the 15 CPO loaded SP formulations generated according to the Box-Behnken experimental design are presented in Table 2. The effects of the formulation variables on VS, PDI, and EE% are discussed in the following sections.

Table 2. Formulations suggested by Box-Behnken model for the CPO SPs and the results of their measured responses (VS, PDI, and EE%).

	Factor 1 (X1)	**Factor 2 (X2)**	**Factor 3 (X3)**	**Response 1 (Y1)**	**Response 2 (Y2)**	**Response 3 (Y3)**
F	Conc. of Span 60 (mg/mL)	Conc. of Tween 80 (mg/mL)	Sonication time (min.)	VS (nm)	PDI	EE%
F1	20	10	2.5	100.8	0.25	83.2
F2	60	10	2.5	665.6	0.32	82.6
F3	20	40	2.5	16.4	0.21	80.4
F4	60	40	2.5	127.3	0.32	79.1
F5	40	10	0	236.7	0.27	90.0
F6	60	25	0	883.2	0.33	91.5
F7	20	25	5	28.6	0.23	90.1
F8	60	25	5	242.5	0.29	90.3
F9	20	25	0	165.3	0.27	92.7
F10	40	40	5	117.0	0.26	87.0
F11	40	10	5	219.0	0.25	86.0
F12	40	40	0	289.1	0.28	89.3
F13	40	25	2.5	148.6	0.23	91.1
F14	40	25	2.5	148.2	0.25	90.9
F15	40	25	2.5	148.0	0.24	90.1

Note: The concentration of CPO in all formulations is 20 mg/mL. The data are expressed as mean ± SD.

3.1.1.1. Effect on vesicle size

The vesicle size of SP formulations was significantly influenced by the concentration of Span 60, the concentration of Tween 80, and the sonication time. Regarding the concentration of Span 60 (Factor 1), a higher concentration of Span 60 generally resulted in larger vesicles. For instance, formulation F2 containing 60 mg/mL of Span 60 demonstrated a vesicle size of 665.6 nm, whereas F1 prepared with 20 mg/mL showed a size of 100.8 nm, as shown in Table 2. This increase in vesicle size can be attributed to the higher concentration of the vesicle-forming surfactant, which promotes the formation of larger bilayer structures and consequently increases vesicle size [38].

While, increasing the concentration of Tween 80 (Factor 2), reduced the vesicle size, particularly at lower Span 60 concentrations. This effect is obvious when comparing F3 formulation, containing 40 mg/mL of Tween 80 with a vesicle size of 16.48 nm, with F1 containing 10 mg/mL, which showed a size of 100.8 nm. Tween 80 acts as an edge activator which reduces the interfacial tension and enhances vesicle flexibility leading to the formation of smaller and more deformable vesicles [39]. However, this size-reducing effect became less pronounced at higher Span 60 concentrations, indicating an interaction between Factors 1 and 2.

Concerning the effect of the sonication time (Factor 3), a longer sonication time of 5 minutes decreased the vesicle size owing to the intense cavitation forces generated during sonication, which fragment larger vesicles into smaller and more uniformly dispersed ones. For example, F7 formulation, prepared with a sonication time of 5 minutes has a vesicle size of 28.67 nm. Whereas F9, prepared without sonication, showed a vesicle size of 165.3 nm. Sonication provides energy for homogenisation, leading to smaller and more uniform vesicles [28]. Overall, the findings indicate that vesicle size was influenced by combined effect of Span 60 concentration, Tween 80 concentration, and sonication duration, that need to be carefully manipulated to obtain the optimised formulation.

3.1.1.2. Effect on polydispersity index

As can be observed in Table 2, the PDI of the SPs formulations was influenced mainly by the concentration of Span 60 (Factor 1) and the sonication time (Factor 3). Formulations prepared with low and intermediate concentrations of Span 60 (20 and 40 mg/mL) generally exhibited lower PDI values, indicating a narrower vesicle size distribution and greater formulation homogeneity. In contrast, increasing the amount of Span 60 to 60 mg/mL resulted in higher PDI values (> 0.30) as shown in formulations F2, F4, and F6, suggesting the formation of a more heterogeneous vesicle population.

Sonication also played an important role in improving vesicle uniformity. Increasing the sonication time reduced the PDI values, as demonstrated by formulations prepared with 5 minutes of sonication, owing to the cavitation forces generated during sonication, which break down larger vesicles and produce a more homogeneous vesicle population [29]. For example, formulation F6 (0 minute sonication) exhibited a PDI of 0.33, whereas F8 (5 minute sonication) showed a reduced PDI of 0.29. Similarly, the PDI decreased from 0.27 in F9 to 0.23 in F7 following sonication. In contrast, the concentration of Tween 80 (Factor 2) had only a limited effect on the PDI values within the investigated concentration range, as only minor variations in PDI were observed among the formulations. For example, increasing the Tween 80 concentration from 10 to 40 mg/mL (F2 and F4) resulted in identical PDI values (0.32), indicating that Tween 80 concentration had little effect on vesicle size distribution under these experimental conditions. Overall, the PDI values (0.21–0.33) indicate that the formulations exhibited suitable size distributions, necessary for the vesicular drug delivery systems.

3.1.1.3. Effect on entrapment efficiency

The increase in the concentration of Span 60 (Factor 1) from the lowest (20 mg/mL) to the highest concentration (60 mg/mL) had a non-significant effect on the EE%, as observed when comparing EE% values of the formulations F1 and F2 (83.2% and 82.6%), F3 and F4 (80.4% and 79.3%), as well as F7 and F8 (90.1% and 90.3%). However, at the highest Span 60 concentration (60 mg/mL), increasing the concentration of Tween 80 (Factor 2) from 10 mg to 40 mg/mL resulted in a reduction in EE%, as observed when comparing formulations F2 and F4 with an EE% of (82.6% and 79.3%). This finding is in agreement with a study reported by Sabri et al. [29] The higher concentration of Tween 80 (40 mg/mL) may increase the fluidity and deformability of the vesicular bilayer, facilitating drug leakage from the vesicles and consequently reducing the EE% [40]. While the use of an intermediate concentration of Tween 80 (25 mg/mL) has improved the EE%, as demonstrated by formulation F6-F9, F13-F15, which exhibited an EE% of higher than 90%. This improvement may be attributed to an optimal balance between bilayer flexibility and structural integrity, allowing efficient drug entrapment while maintaining vesicle stability. Sonication time (Factor 3) also influenced the EE% of the SPs formulations by interaction with the other factors. Generally, the use of the highest sonication time (5 minutes) resulted in a lower EE% of the same formulation without sonication (zero). For instance, when comparing F8 and F6, F7 and F9, F10 and F12, F11 and F5. This may be due to the leakage of CPO from the vesicles leading to the reduction in the EE% [34]. An intermediate sonication time of (2.5 minutes) with intermediate concentrations of Span 60 (40 mg/mL), and Tween 80 (25 mg/mL) resulted in an enhancement of the EE% (> 90%) as noticed in F13-F15. This could be attributed to improving drug distribution within the vesicles resulted from the better interaction between the three factors. Overall, the findings indicate that the EE% was mainly influenced by the Tween 80 concentration and sonication duration, while Span 60 concentration had no notable effect within the tested experimental parameters.

3.1.2. Optimisation of spanlastics vesicles

Numerical optimisation was employed to predict the optimum formulation parameters for CPO SPs vesicles, targeting minimised VS and PDI alongside maximised EE% aiming to achieve a desirability value approaching 1. Based on the response surface analysis evaluating the impact of independent variables on the measured responses, the Design-Expert software generated several potential solutions. Among these, Solution 1 achieved the highest overall desirability value of 0.921 as shown in Figure 2A. The predicted optimised formulation consisted of 20 mg of Span 60, 25 mg of Tween 80, with a sonication time of 1.8-minute as illustrated in Figure 2B. This formulation was subsequently prepared and experimentally validated as the optimised formulation for further characterisation and evaluation.

To assess the predictive ability of the Box-Behnken model, the percentage error was determined by comparing the predicted values of the VS, PDI, and EE% generated by the model with actual experimental values of the optimised formulation. As shown in Table 3, the results of the percentage error for all responses were below 5%, indicating the good agreement between the predicted and experimental values. This confirms the adequate reliability of the Box-Behnken model for optimisation of the SP formulations.

Table 3. The values and the error % of the variables (VS, PDI, and EE%) for the predicted and actual optimised formulation. Actual values were measured in triplicate and presented as the mean ± SD.

Variable	Predicted values	Actual values	% Error
VS	149.38	145.63 ± 6.51	2.51
PDI	0.24	0.25 ± 0.02	4.16
EE%	92.62	91.51 ± 0.33	1.19

3.1.3. Measurement of zeta potential

The zeta potential of the optimised CPO SP formulation was determined to evaluate its stability. The measured value was −20.9 ± 1.3 mV; this result indicates a moderate stability of the nanosystem. In general, zeta potential values of approximately 20–30 mV are considered sufficient to provide moderate electrostatic stabilisation, thereby reducing the tendency of vesicles to aggregate. The observed negative surface charge is likely due to the adsorption of hydroxyl ions from the aqueous medium and the orientation of oxygen-containing groups at the vesicle surface. In addition, CPO is weakly acidic drug and the ionisation behaviour at the formulation pH may also contribute to the overall surface charge. These findings are consistent with previous studies on SPs which reported zeta potential ranging from −15 to −30 mV, depending on surfactant composition of the vesicles [40]. Similarly, Tween 80 based nanovesicles exhibited zeta potential of around −22 mV which is in good agreement with the present findings. Therefore, the obtained zeta potential value suggests adequate stability of the SP vesicles and is expected to remain well dispersed without significant aggregation during storage period.

3.1.4. Transmission Electron Microscopy (TEM)

As shown in Figure 3, the vesicles were predominantly spherical to near-spherical in shape. A small proportion of vesicles exhibited slight deformation and localised aggregation, which are commonly observed in TEM analyses of nanovesicular systems. These morphological variations are most likely attributable to sample preparation procedures, including dehydration, air-drying, and negative staining, which may induce vesicle shrinkage, flattening, partial collapse, or overlap between adjacent vesicles during solvent evaporation. Consequently, the observed aggregates are considered preparation-induced artifacts rather than evidence of poor colloidal stability. Similar spherical or near-spherical vesicles with occasional deformation or aggregation resulting from sample preparation have been reported previously for SPs formulations [21, 41].

3.1.5. *In vitro* antifungal activity study

The agar well diffusion assay demonstrated significant differences in the antifungal activities of the tested formulations. As shown in Figure 4, the optimised CPO SP formulation exhibited the largest zone of inhibition (ZOI) (35 ± 0.25 mm), which was significantly greater than that produced by CPO dissolved in DMSO (31 ± 0.35 mm). In contrast, the blank SP formulation

produced no detectable inhibition zone, confirming that the antifungal activity was solely attributable to CPO rather than the SP carrier. These findings are in agreement with those reported by Ansari et al. [23].

The significantly larger inhibitory zone of CPO SPs may be due to many reasons, including the ability of SPs to enhance the solubility and improve the aqueous dispersibility of CPO, resulting in improved diffusion through the agar medium. In addition, the deformable vesicular structure of the SPs increases the available surface area of the drug and promotes closer interaction with fungal cells, thereby enhancing antifungal efficacy. Conversely, although CPO dissolved in DMSO exhibited considerable antifungal activity, it lacks the drug delivery advantages offered by the SPs carrier. The relatively large inhibition zone observed for the DMSO solution may be explained by the excellent solvent properties of DMSO, which facilitate drug dissolution and diffusion within the agar matrix. Furthermore, DMSO may exhibit a modest intrinsic antifungal activity [42]. Numerous studies demonstrated the improvement in the antifungal activity of drugs following encapsulation in nanocarrier systems [43].

3.2. Characterisation of the prepared spanlastic nanogel

3.2.1. Viscosity measurement

The viscosity values of the SP nanogel formulations (SPNG1, SPNG2, SPNG3, and SPNG4) containing different concentrations of Carbopol 934P (0.25%, 0.5%, 0.75%, and 1%) respectively, are shown in Table 4. It was observed that the viscosity steadily increased with elevated polymer concentration (from 0.25% to 1%) at all tested rotational speeds. This may be due to the formation of a denser polymeric network within the gel matrix. This increase is attributed to the greater number of hydrated polymer chains and enhanced intermolecular hydrogen bonding and chain entanglement, which increase the resistance of the gel to flow. Other studies have also reported the rise in value of viscosity measured with the increase in Carbopol concentration[44]. All formulations exhibited a decrease in viscosity with increasing rotational speed, indicating pseudoplastic (shear-thinning) non-Newtonian behaviour, which is characteristic of Carbopol-based hydrogels, where the intermolecular entanglements reduced under shear. Such rheological behaviour is advantageous for topical and transungual formulations because it facilitates easy spreading during application while allowing the formulation to recover its high viscosity after shear removal, thereby improving retention at the application site [45].

Table 4. Viscosity results of different concentrations of CPO SP nanogels.

Rotational speed	Viscosity (cp) SPNG1	Viscosity (cp) SPNG2	Viscosity (cp) SPNG3	Viscosity (cp) SPNG4
10	5400 ± 0.152	19710 ± 0.224	20595 ± 0.244	21860 ± 0.545
12	4720 ± 0.251	18150 ± 0.632	18220 ± 0.155	19840 ± 0.618
20	3550 ± 0.387	12422 ± 0.922	15670 ± 0.309	17430 ± 0.885
30	3020 ± 0.613	9180 ± 0.543	11490 ± 0.604	14880 ± 0.332
50	2890 ± 0.541	6150 ± 0.492	7600 ± 0.312	9040 ± 0.435
60	2235 ± 0.529	5249 ± 0.223	5900 ± 0.498	6330 ± 0.715
100	1950 ± 0.351	3533 ± 0.294	3920 ± 0.445	5419 ± 0.255

3.2.2. Determination of drug content

The results of the measurement of drug content percentage of CPO in SP nanogel formulations SPNG1, SPNG2, SPNG3, and SPNG4 was (99.1 ± 0.2%, 97.3 ± 0.55%, 93.2 ± 1.1%, and 91.3 ± 0.4%), respectively. The high drug content values obtained for all formulations indicate an effective and uniform distribution of the drug in the gel matrix. However, there was a minor reduction in drug content as Carbopol 934P concentration increases, particularly in formulations containing 0.75% and 1% w/w polymer. This may be attributed to the higher viscosity and denser polymer network formed at elevated Carbopol concentrations, which can hinder the homogeneous dispersion of the SP vesicles and reduce the efficiency of drug extraction during analysis. Nevertheless, all formulations exhibited drug contents above 90%, indicating satisfactory drug loading and minimal drug loss during the preparation process [43, 46].

3.2.3. *In vitro* release study

The *in vitro* release profiles of CPO SPs nanogel formulations (SPNG1, SPNG2, SPNG3, and SPNG4) over 12 hours are illustrated in Figure 5. An inverse relationship was observed between the concentration of Carbopol 934P and the cumulative drug release percentage. Formulation SPNG1, containing 0.25% w/w Carbopol 934P, exhibited the highest cumulative drug release (80.37 ± 1.65%) after 12 hours, whereas SPNG4, containing 1.0% w/w Carbopol 934P, showed the lowest cumulative release (32.5 ± 2.54%). These findings indicate that increasing the polymer concentration effectively retarded the release of CPO from the nanogel matrix. The reduction in drug release with increasing Carbopol 934P concentration can be attributed to the formation of a denser and more viscous three-dimensional polymeric network, which increases the diffusional resistance encountered by drug molecules. Carbopol 934P is a cross-linked polyacrylic acid polymer that exhibits high viscosity and forms a dense gel network. As the concentration of Carbopol 934P increases, both the gel viscosity and the diffusional barrier become more pronounced, which impedes drug release. Elevated polymer concentration results in dense polymeric entanglements, thereby reducing drug diffusion from the nanogel matrix [51]. Among the investigated formulations, SPNG1 demonstrated the most favourable release profile, providing prolonged drug release over the 12 hours experimental period while maintaining higher cumulative release than the formulations containing higher polymer concentrations. Therefore, SPNG1 was selected as the optimum nanogel formulation for subsequent investigations.

3.2.4. Measurement of the vesicle size, polydispersity index, and zeta potential

The optimum SP nanogel formulation (SPNG1) showed an average vesicle size of 241.4 ± 1.13 nm as demonstrated in Figure 6A. This value was higher than the vesicle size of the optimised SPs formulation, which exhibited a vesicle size of 145.3 ± 2.66 nm. This increase in the vesicle size of the SP nanogel following the use of Carbopol 934P as a gelling agent can be attributed to the increase in the hydrodynamic diameter resulting from the adsorption or association of hydrated polymer chains around the SP vesicles [47, 48].

The PDI value of the optimised SPs formulation was 0.276 ± 0.02, whereas the corresponding nanogel (SPNG1) showed a slightly lower PDI of 0.270 ± 0.01. This indicates that the incorporation of the SP vesicles into the Carbopol gel did not adversely affect their size distribution and suggests that the vesicles remained uniformly dispersed within the gel matrix. The gel matrix may prevent particle aggregation, leading to a more homogeneous dispersion. The polymer network could restrict the movement of vesicles in the formulation and result in reducing size variability in DLS measurements [32].

The zeta potential of the CPO SPs nanogel formulation (SPNG1) was measured to evaluate its stability. As shown in Figure 6B, the formulation exhibited a zeta potential of −29.8 ± 0.85 mV. This indicates good colloidal stability and a more negative surface charge than the original CPO SPs of −20.9 ± 1.2 mV. The increase in the absolute magnitude of the negative zeta potential following gel incorporation may be due to an increase in the negative charge density because of the presence of Carbopol 934P that ionises in water and contributes additional carboxylate ($-COO^-$) groups [49].The enhanced negative surface charge, together with the steric stabilisation provided by the nonionic surfactant Tween 80, contributes to reducing vesicle aggregation and maintaining good colloidal stability. In addition, the three-dimensional Carbopol gel network restricts vesicle mobility, further improving the physical stability of the formulation. Similar zeta potential values ranging from −20 to −35 mV have been reported for Carbopol-based nanogel formulations, confirming that the obtained value is consistent with a physically stable nanosystem suitable for topical drug delivery [50].

3.2.5. Field Emission Scanning Electron Microscopy (Fe-SEM)

The Fe-SEM examination of the optimised formulation (SPNG1) showed spherical to ovoid vesicles with smooth surfaces as illustrated in Figure 7. The vesicles appeared well dispersed, with no obvious evidence of extensive aggregation, suggesting that incorporation of the SP vesicles into the Carbopol gel maintained good physical stability. These results are in agreement with previous findings from similar research on SPs nanovesicles, which also documented the spherical shape and uniform size distribution of SPs [52].

3.2.6. *Ex vivo* permeation study

As previously mentioned, the *ex vivo* permeation was carried out using both sheep hooves and healthy human fingernails to compare the permeation of the optimum SPs nanogel formulation (SPNG1) with the corresponding plain gel. Healthy nail plates were selected because previous studies have reported that the permeability of healthy nails is comparable to that of fungal-infected nails, making healthy nails a suitable and widely accepted model for *ex vivo* transungual permeation studies [53].

3.2.6.1. Permeation study using sheep hooves

Sheep hooves are widely accepted as a practical *ex vivo* model for the initial evaluation of transungual drug delivery due to their structural similarities (keratinised tissue) and greater availability than human nails [54, 55]. Although structural differences between sheep hooves and human nails may influence the extent of drug permeation, sheep hooves remain a well-established model for comparative formulation studies. As illustrated in Figure 8A, the optimum SP nanogel formulation (SPNG1) showed significantly greater drug deposition within the sheep hooves than the corresponding plain gel (450.5 ± 4.09 versus 292.01 ± 1.75 μg/cm², respectively; $P < 0.001$), representing approximately a 1.54-fold increase in drug deposition. Likewise, the cumulative amount of CPO permeated into the receptor fluid after 24 hours was significantly higher for the SP nanogel (161.73 ± 2.01 μg/cm²) than for the plain gel (112.10 ± 0.93 μg/cm²) ($P < 0.001$). The superior transungual delivery accomplished by the SP nanogel may be due to their highly deformable nature, which increases their interaction with keratin and enables drug diffusion through the tissue.

3.2.6.2. Permeation study using human nails

According to the permeation study results, the optimum SP nanogel formulation (SPNG1) showed a higher permeation and deposition within the human fingernails than the corresponding plain gel. As shown in Figure 8B, the amount of CPO retained within the nails after 24 hours was 269.1 ± 0.95 μg/cm² for the SP nanogel compared with 155.3 ± 2.05 μg/cm² for the plain gel, representing approximately a 1.73-fold increase in drug deposition ($P < 0.001$). In addition, the cumulative amount of drug permeated into the receptor fluid after 24 hours was significantly higher for the SP nanogel (37.8 ± 1.12 μg/cm²) than for the plain gel (24.34 ± 1.09 μg/cm²) ($P < 0.001$).

The greater drug deposition achieved by the SPNG1 formulation is important for the treatment of onychomycosis, since dermatophytes colonize the nail plate and the underlying nail bed. Thus, increasing drug retention within the nail is regarded more critical than achieving higher systemic permeation. The high level of drug deposition observed for the SP nanogel is expected to maintain prolonged local drug availability within the nail tissue, thereby supporting sustained antifungal activity [56, 57].

The superiority of SP nanogel in improving transungual drug delivery may be attributed to several mechanisms. First, the non-ionic surfactants (Span 60 and Tween 80) act as permeation enhancers by increasing hydration of the keratinised nail plate and facilitating drug diffusion through the compact keratin network [58, 59]. Second, the nanosized and highly deformable SP vesicles can adapt their shape and traverse the aqueous pathways within the hydrated keratin tissue more efficiently than do the plain gel. In addition, the vesicles may adsorb onto the nail surface and function as localised drug reservoirs, providing continuous release of CPO directly at the site of permeation. Together, these mechanisms resulted in significantly greater drug deposition and permeation than those attained with the plain gel.

3.2.7. Pre-treatment with MN pen device

Microneedle-assisted transungual drug delivery systems utilises arrays of microscopic needles to create micropores in the nail plate. Thus, reducing the barrier function of the highly keratinised tissue without reaching pain receptors [59]. Furthermore, the formation of numerous micropores increases the effective surface area available for drug transport, thereby facilitating diffusion through the keratin matrix [76]. Consequently, this minimally invasive technique enhances drug permeation while remaining painless. The pre-treatment of the sheep hooves or human nails with the MN pen device has shown a synergistic effect and significantly increased permeation and deposition of CPO from both SP nanogel and the plain gel, as shown in Figure 9.

As shown in Figure 9, MN pre-treatment showed a significant increase in the CPO amount deposited in both samples. In sheep hooves, drug deposition increased from 450.5 ± 4.09 to 791.03 ± 1.95 μg/cm² (76% increase) for the SP nanogel and from 292.01 ± 1.75 to 385.6 ± 9.25 μg/cm² (32% increase) for the plain gel. Likewise, in human nails, the drug deposition from the SPs nanogel increased from 269.1 ± 0.95 to 417.0 ± 2.55 μg/cm² (55% increase), whereas the plain gel increased from 155.3 ± 2.05 to 176.16 ± 6.05 μg/cm² (13% increase).

Regarding the permeation of CPO into the receptor fluid, notable increase also observed. In sheep hooves, receptor-fluid permeation increased from 161.73 ± 2.01 to 210.32 ± 1.17 μg/cm² (30% increase) for the SP nanogel, and from 112.10 ± 0.93 to 139.72 ± 0.06 μg/cm² (24.6% increase) for the plain gel. MN pre-treatment of the human nails increased CPO permeation

from 37.8 ± 1.12 to 45.79 ± 0.08 μg/cm² (22% increase) for the SP nanogel, and from 24.34 ± 1.09 to 28.55 ± 0.35 μg/cm² (17.3% increase) for the plain gel.

The significant enhancement of the MN pen device detected with the SP nanogel indicates a synergistic action between MN-assisted microporation and the SP nanovesicles. While the MN pen physically reduces the diffusional resistance of the keratinized barrier of the nail by creating microchannels, the highly deformable SPs easily penetrate these newly formed pathways and subsequently diffuse more efficiently through the hydrated keratin matrix. In addition, the nanosized vesicles maintain CPO in a finely dispersed state and facilitate its partitioning into the nail tissue, resulting in greater drug deposition and permeation than those achieved with the conventional plain gel. These complementary mechanisms explain the superior performance of the combined MN-SP nanogel approach [60, 61].

Transungual drug delivery was observed to be higher in sheep hooves than in human nails following MN pre-treatment. These differences may be due to the structural properties of sheep hooves, including their lower keratin density, higher lipid content, and greater water absorption capacity compared with human nails. Increased hydration promotes swelling of the keratin network and enlargement of aqueous diffusion pathways, thereby facilitating drug transport. Although the absolute permeation values differed between the two models (hooves and nails), the same enhancement pattern was consistently observed, demonstrating that the synergistic effect of MN-assisted microporation and SP nanovesicles is independent of the keratin substrate. Finally, the noticeable increase in drug deposition within the nail plate is particularly relevant for the treatment of onychomycosis, where fungi reside primarily within the keratinized tissue. Therefore, combining MN-assisted microporation with CPO-loaded SP nanogel has the potential to increase local drug availability and may shorten treatment duration compared with conventional topical therapy.

3.2.8. Stability study of spanlastics nanogel

The stability of CPO SP nanogel formulation (SPNG1) was evaluated over a period of three months at 4°C, 25°C, and 40°C by monitoring vesicle size, PDI, pH, and drug content. The results are presented in Table 5.

At 4°C storage for a period of three months, the vesicle size was gradually increased from 248.5 ± 0.95 nm to 298.5 ± 2.45 nm, this increase indicates a limited aggregation of vesicles. The reduced growth rate of the vesicles with decreased molecular mobility and inhibited coalescence under refrigerated conditions. At a storage temperature of 25°C, a notable increase in size was recorded, reaching 466.2 ± 1.45 nm after three months, suggesting a reduction in stability at ambient temperature. The highest increase in the vesicle size occurred at 40°C, where it reached 2247.0 ± 7.45 nm, indicating extensive vesicle aggregation and/or fusion induced by higher temperature. Higher temperatures increase bilayer fluidity and vesicle mobility, thereby promoting collisions between vesicles and reducing the physical stability of the nanosystem [59].

The PDI of a freshly prepared nanogel was 0.270 ± 0.01, indicating a homogeneous size distribution, which is advantageous for consistent drug delivery. Following the storage at 4°C and 25°C for three months, the PDI values remained low (0.268 ± 0.04, and 0.232 ± 0.02, respectively), indicating maintained homogeneity despite droplet enlargement. This elucidates that aggregation occurred without high effect on the size variation. At 40°C, the PDI increased to 0.350 ± 0.01. This reflects the development of a larger size distribution due to increased aggregation at elevated temperature.

The pH of the nanogel remained relatively stable throughout the storage period, increasing only slightly from 7.40 ± 0.02 to 7.68 ± 0.03 after three months at 40°C. This is important for preserving nail compatibility and drug stability, as CPO deteriorates under excessively acidic or alkaline conditions [56].

The drug content values of the CPO SP nanogel decreasing only slightly from 99.1 ± 0.20% in the freshly prepared formulation to 96.9 ± 1.21% after three months at 40°C. The slight loss in drug content (< 3%) indicates good chemical stability of CPO within the SP nanogel. The small decrease in drug content at high temperatures may be attributed to minor drug leakage from the vesicles and/or gradual thermal degradation during storage [62].

Table 5. Results of the stability study of CPO SP nanogel. The data are presented as mean ± SD (n = 3).

Temp.	Time (month)	Vesicle size (nm)	PDI	pH	Drug content %
	0	241.4 ± 1.13	0.270 ± 0.01	7.40 ± 0.02	99.1 ± 0.20
4°C	1	248.5 ± 0.95	0.237 ± 0.03	7.43 ± 0.02	99.1 ± 0.39

	2	284.1 ± 4.50	0.242 ± 0.01	7.51 ± 0.01	98.9 ± 0.55
	3	298.5 ± 2.45	0.268 ± 0.04	7.62 ± 0.01	98.6 ± 0.45
25°C	1	302.7 ± 2.08	0.208 ± 0.03	7.63 ± 0.02	99.0 ± 0.22
	2	427.2 ± 1.75	0.230 ± 0.03	7.62 ± 0.01	98.7 ± 1.46
	3	466.2 ± 1.45	0.232 ± 0.02	7.65 ± 0.03	97.9 ± 0.62
40°C	1	798.0 ± 5.05	0.366 ± 0.03	7.64 ± 0.04	98.1 ± 0.15
	2	1471.5 ± 2.55	0.370 ± 0.01	7.65 ± 0.02	97.8 ± 0.29
	3	2247.0 ± 7.45	0.350 ± 0.01	7.68 ± 0.03	96.9 ± 1.21

4. CONCLUSIONS

The current work successfully developed and optimised an innovative topical SPs formulation of the antifungal agent CPO using a Box–Behnken experimental design. The optimised formulation exhibited nanosized vesicles with high drug entrapment efficiency and enhanced antifungal activity compared with the free drug formulation. The SPs were then successfully incorporated into a Carbopol-based gel which showed suitable viscosity, drug content, drug release, and stability under refrigerated storage. *Ex vivo* permeation studies using both sheep hooves and human fingernails demonstrated that the SP nanogel significantly increased drug permeation and drug deposition within the hooves and nails compared with the corresponding plain gel. Pre-treatment with a MN pen device further enhanced transungual drug delivery, demonstrating a synergistic effect between MN-assisted nail microporation and the highly deformable SP nanovesicles. The combined approach produced the greatest drug deposition within the nail plate, which is beneficial for the topical treatment of onychomycosis, where sustained drug retention within the nail is essential for therapeutic efficacy. Overall, the developed SP nanogel, particularly when combined with MNs, provides a promising strategy for improving topical antifungal therapy and overcoming the barrier properties of the nail plate. Nevertheless, further *in vivo* studies are required to confirm the therapeutic efficacy and clinical applicability of this novel transungual drug delivery system.

REFERENCES

[1] Muralidhar P, Bhargav E, Reddy R. Transungual drug delivery: an over view. Int J Pharma Res Heal Sci. 2017;5:1522-8. doi: DOI:10.21276/ijprhs.2017.01.01.

[2] Tan ES, Chong W-S, Tey HL. Nail psoriasis: a review. American journal of clinical dermatology. 2012;13(6):375-88. doi: https://doi.org/10.2165/11597000-000000000-00000.

[3] Dawber RP. The ultrastructure and growth of human nails. Archives of Dermatological Research. 1980;269(2):197-204. doi: https://doi.org/10.1007/BF00406540.

[4] Piraccini BM, Baran R, Tosti A. Nail disorders: a practical guide to diagnosis and management: Springer; 2014.

[5] Iorizzo M, Starace M, Pasch MC. Leukonychia: what can white nails tell us? American Journal of Clinical Dermatology. 2022;23(2):177-93. doi: https://doi.org/10.1007/s40257-022-00671-6.

[6] Gupta A, Stec N, Summerbell R, Shear N, Piguet V, Tosti A, et al. Onychomycosis: a review. Journal of the European Academy of Dermatology and Venereology. 2020;34(9):1972-90. doi: https://doi.org/10.1111/jdv.16394.

[7] Heikkilå H, Stubb S. The prevalence of onychomycosis in Finland. British Journal of Dermatology. 1995;133(5):699-703. doi: https://doi.org/10.1111/j.1365-2133.1995.tb02741.x.

[8] Alessandrini A, Starace M, Bruni F, Piraccini BM. An open study to evaluate effectiveness and tolerability of a nail oil composed of vitamin E and essential oils in mild to moderate distal subungual onychomycosis. Skin appendage disorders. 2020;6(1):14-8. doi: https://doi.org/10.1159/000503305.

[9] Goldstein AO, Bhatia N. Onychomycosis: management. UpToDate Waltham, MA(Accessed on June 30, 2019). 2022.

[10] Murthy SN, Maibach HI. Topical nail products and ungual drug delivery: CRC press; 2012.

[11] Walters KA, Flynn GL, Marvel JR. Penetration of the human nail plate: the effects of vehicle pH on the permeation of miconazole. Journal of pharmacy and pharmacology. 1985;37(7):498-9. doi: https://doi.org/10.1111/j.2042-7158.1985.tb03050.x.

[12] Abobakr FE, Fayez SM, Elwazzan VS, Sakran W. Effect of different nail penetration enhancers in solid lipid nanoparticles containing terbinafine hydrochloride for treatment of onychomycosis. AAPS PharmSciTech. 2021;22(1):33. doi: https://doi.org/10.1208/s12249-020-01893-9.

[13] Hao J, Smith KA, Li SK. Chemical method to enhance transungual transport and iontophoresis efficiency. International journal of pharmaceutics. 2008;357(1-2):61-9. doi: https://doi.org/10.1016/j.ijpharm.2008.01.027.

[14] Baran R, Hay RJ, Garduno JI. Review of antifungal therapy and the severity index for assessing onychomycosis: part I. Journal of Dermatological Treatment. 2008;19(2):72-81. doi: https://doi.org/10.1080/09546630701243418.

[15] Bet DL, Reis ALd, Chiacchio ND, Belda W. Dermoscopy and onychomycosis: guided nail abrasion for mycological samples. Anais Brasileiros de Dermatologia. 2015;90(6):904-6. doi: https://doi.org/10.1590/abd1806-4841.20154615.

[16] Subissi A, Monti D, Togni G, Mailland F. Ciclopirox: recent nonclinical and clinical data relevant to its use as a topical antimycotic agent. Drugs. 2010;70(16):2133-52. doi: https://doi.org/10.2165/11538110-000000000-00000.

[17] Kokjohn K, Bradley M, Griffiths B, Ghannoum M. Evaluation of in vitro activity of ciclopirox olamine, butenafine HCl and econazole nitrate against dermatophytes, yeasts and bacteria. Int J Dermatol. 2003;42 Suppl 1(S1):11-7. Epub 2003/08/05. doi: 10.1046/j.1365-4362.42.s1.4.x. PubMed PMID: 12895182.

[18] Niewerth M, Kunze D, Seibold M, Schaller M, Korting HC, Hube B. Ciclopirox olamine treatment affects the expression pattern of Candida albicans genes encoding virulence factors, iron metabolism proteins, and drug resistance factors. Antimicrobial agents and chemotherapy. 2003;47(6):1805-17. doi: https://doi.org/10.1128/aac.47.6.1805-1817.2003.

[19] Mucha P, Borkowski B, Erkiert-Polguj A, Budzisz E. Ciclopirox and ciclopirox olamine: antifungal agents in dermatology with expanding therapeutic potential. Applied Sciences. 2024;14(24):11859. doi: https://doi.org/10.3390/app142411859.

[20] Ratnavel RC, Squire RA, Boorman GC. Clinical efficacies of shampoos containing ciclopirox olamine (1.5%) and ketoconazole (2.0%) in the treatment of seborrhoeic dermatitis. J Dermatolog Treat. 2007;18(2):88-96. Epub 2007/05/24. doi: 10.1080/16537150601092944. PubMed PMID: 17520465.

[21] Kakkar S, Kaur IP. Spanlastics—A novel nanovesicular carrier system for ocular delivery. International journal of pharmaceutics. 2011;413(1-2):202-10. doi: https://doi.org/10.1016/j.ijpharm.2011.04.027.

[22] Mosallam S, Albash R, Abdelbari MA. Advanced vesicular systems for antifungal drug delivery. AAPS PharmSciTech. 2022;23(6):206. doi: https://doi.org/10.1208/s12249-022-02357-y.

[23] Ansari MD, Solanki P, Pandit J, Jahan RN, Aqil M, Sultana Y. Fabrication and optimization of raloxifene loaded spanlastics vesicle for transdermal delivery. Journal of Drug Delivery Science and Technology. 2022;68:103102. doi: https://doi.org/10.1016/j.jddst.2022.103102.

[24] Tayel SA, El-Nabarawi MA, Tadros MI, Abd-Elsalam WH. Duodenum-triggered delivery of pravastatin sodium via enteric surface-coated nanovesicular spanlastic dispersions: development, characterization and pharmacokinetic assessments. International journal of pharmaceutics. 2015;483(1-2):77-88. doi: https://doi.org/10.1016/j.ijpharm.2015.02.012.

[25] Abdelbari MA, El-Mancy SS, Elshafeey AH, Abdelbary AA. Implementing spanlastics for improving the ocular delivery of clotrimazole: in vitro characterization, ex vivo permeability, microbiological assessment and in vivo safety study. International journal of nanomedicine. 2021;16:6249-61. doi: https://doi.org/10.2147/IJN.S319348.

[26] Alhammid SNA, Kassab HJ, Hussein LS, Haiss MA. Spanlastics nanovesicles: An emerging and innovative approach for drug delivery. Maaen Journal for Medical Sciences. 2023;2(2):9. doi: https://doi.org/10.55810/2789-9136.1027.

[27] Abdulnabi AA, Ali KF, Abd Razik BM. Synthesis, Characterization, ADME Study and Antimicrobial Evaluation of New 1, 2, 3-triazole Derivatives of 2-phenyl benzimidazole. Al Mustansiriyah Journal of Pharmaceutical Sciences. 2023;23(2):147-57. doi: https://doi.org/10.32947/ajps.v23i2.1016.

[28] Alharbi WS, Hareeri RH, Bazuhair M, Alfaleh MA, Alhakamy NA, Fahmy UA, et al. Spanlastics as a potential platform for enhancing the brain delivery of flibanserin: in vitro response-surface optimization and in vivo pharmacokinetics assessment. Pharmaceutics. 2022;14(12):2627. doi: https://doi.org/10.3390/pharmaceutics14122627.

[29] Al-mansoori MK, Sabri LA. Preparation and evaluation of transdermal gel loaded with spanlastics containing meloxicam. Journal of Research in Pharmacy. 2024;28(4):1200-9. doi: http://dx.doi.org/10.29228/jrp.801

[30] Saleh A, Khalifa M, Shawky S, Bani-Ali A, Eassa H. Zolmitriptan intranasal spanlastics for enhanced migraine treatment; formulation parameters optimized via quality by design approach. Scientia pharmaceutica. 2021;89(2):24. doi: https://doi.org/10.3390/scipharm89020024.

[31] Ibrahim MS, Elkady OA, Amer MA, Noshi SH. Exploiting response surface D-optimal design study for preparation and optimization of spanlastics loaded with miconazole nitrate as a model antifungal drug for topical application. Journal of Pharmaceutical Innovation. 2023;18(4):2402-18. doi: https://doi.org/10.1007/s12247-023-09800-y.

[32] Zheng Y, Ouyang W-Q, Wei Y-P, Syed SF, Hao C-S, Wang B-Z, et al. Effects of Carbopol® 934 proportion on nanoemulsion gel for topical and transdermal drug delivery: A skin permeation study. International journal of nanomedicine. 2016;11:5971-87. doi: https://doi.org/10.2147/IJN.S119286.

[33] Khazaeli P, Pardakhty A, Shoorabi H. Caffeine-loaded niosomes: characterization and in vitro release studies. Drug Deliv. 2007;14(7):447-52. Epub 2007/11/13. doi: 10.1080/10717540701603597. PubMed PMID: 17994362.

[34] Dahash RA, Ghareeb MM. Design, Development, and Optimization of Spanlastics for Delivery of Rizatriptan Benzoate. Iraqi Journal of Pharmaceutical Sciences. 2025;34(4):125-40. doi: https://doi.org/10.31351/vol34iss4pp125-140.

[35] Mertin D, Lippold BC. In-vitro permeability of the human nail and of a keratin membrane from bovine hooves: Influence of the partition coefficient octanol/water and the water solubility of drugs on their permeability and maximum flux. Journal of pharmacy and pharmacology. 1997;49(1):30-4. doi: https://doi.org/10.1111/j.2042-7158.1997.tb06747.x.

[36] Al-Badry AS, Al-Mayahy MH, Scurr DJ. Enhanced transdermal delivery of acyclovir via hydrogel microneedle arrays. Journal of Pharmaceutical Sciences. 2023;112(4):1011-9. doi: https://doi.org/10.1016/j.xphs.2022.11.012.

[37] Al-Mayahy MH, Sabri AH, Rutland CS, Holmes A, McKenna J, Marlow M, et al. Insight into imiquimod skin permeation and increased delivery using microneedle pre-treatment. European Journal of Pharmaceutics and Biopharmaceutics. 2019;139:33-43. doi: https://doi.org/10.1016/j.ejpb.2019.02.006.

[38] Junyaprasert VB, Singhsa P, Suksiriworapong J, Chantasart D. Physicochemical properties and skin permeation of Span 60/Tween 60 niosomes of ellagic acid. International journal of pharmaceutics. 2012;423(2):303-11. doi: https://doi.org/10.1016/j.ijpharm.2011.11.032.

[39] Alaaeldin E, Abou-Taleb HA, Mohamad SA, Elrehany M, Gaber SS, Mansour HF. Topical nano-vesicular spanlastics of celecoxib: enhanced anti-inflammatory effect and down-regulation of TNF-α, NF-κB and COX-2 in complete Freund's adjuvant-induced arthritis model in rats. International Journal of Nanomedicine. 2021;16:133-45. doi: https://doi.org/10.2147/IJN.S289828.

[40] Salem HF, Kharshoum RM, Abou-Taleb HA, Farouk HO, Zaki RM. Fabrication and appraisal of simvastatin via tailored niosomal nanovesicles for transdermal delivery enhancement: In vitro and in vivo assessment. Pharmaceutics. 2021;13(2):138. doi: https://doi.org/10.3390/pharmaceutics13020138.

[41] El Zaafarany GM, Awad GA, Holayel SM, Mortada ND. Role of edge activators and surface charge in developing ultradeformable vesicles with enhanced skin delivery. International journal of pharmaceutics. 2010;397(1-2):164-72. doi: https://doi.org/10.1016/j.ijpharm.2010.06.034.

[42] Randhawa MA. The effect of dimethyl sulfoxide (DMSO) on the growth of dermatophytes. Nippon Ishinkin Gakkai Zasshi. 2006;47(4):313-8. doi: https://doi.org/10.3314/jjmm.47.313.

[43] Sarfraz RM, Khan MU, Mahmood A, Akram MR, Minhas MU, Qaisar MN, et al. Synthesis of co-polymeric network of carbopol-g-methacrylic acid nanogels drug carrier system for gastro-protective delivery of ketoprofen and its evaluation. Polymer-Plastics Technology and Materials. 2020;59(10):1109-23. doi: https://doi.org/10.1080/25740881.2020.1719148.

[44] Andrews GP, Jones DS. Rheological characterization of bioadhesive binary polymeric systems designed as platforms for drug delivery implants. Biomacromolecules. 2006;7(3):899-906. doi: https://doi.org/10.1021/bm050620y.

[45] Bonacucina G, Cespi M, Misici-Falzi M, Palmieri GF. Rheological, adhesive and release characterisation of semisolid Carbopol/tetraglycol systems. International Journal of Pharmaceutics. 2006;307(2):129-40. doi: https://doi.org/10.1016/j.ijpharm.2005.09.034.

[46] Delgado-Pujol EJ, Martínez G, Casado-Jurado D, Vázquez J, León-Barberena J, Rodríguez-Lucena D, et al. Hydrogels and nanogels: pioneering the future of advanced drug delivery systems. Pharmaceutics. 2025;17(2):215. doi: https://doi.org/10.3390/pharmaceutics17020215.

[47] Siepmann J, Göpferich A. Mathematical modeling of bioerodible, polymeric drug delivery systems. Advanced drug delivery reviews. 2001;48(2-3):229-47. doi: https://doi.org/10.1016/S0169-409X(01)00116-8.

[48] Abdelkader H, Alani AW, Alany RG. Recent advances in non-ionic surfactant vesicles (niosomes): self-assembly, fabrication, characterization, drug delivery applications and limitations. Drug delivery. 2014;21(2):87-100. doi: https://doi.org/10.3109/10717544.2013.838077.

[49] Patil A, Kontamwar P. Formulation and evaluation of antifungal nanogel for topical drug delivery system. Asian J Pharm Clin Res. 2021;14:127-34. doi: http://dx.doi.org/10.22159/ajpcr.2021v14i10.42421.

[50] Prabhakar K, Afzal SM, Surender G, Kishan V. Tween 80 containing lipid nanoemulsions for delivery of indinavir to brain. Acta Pharmaceutica Sinica B. 2013;3(5):345-53. doi: https://doi.org/10.1016/j.apsb.2013.08.001.

[51] Elmowafy E, El-Gogary RI, Ragai MH, Nasr M. Novel antipsoriatic fluidized spanlastic nanovesicles: In vitro physicochemical characterization, ex vivo cutaneous retention and exploratory clinical therapeutic efficacy. International journal of pharmaceutics. 2019;568:118556. doi: https://doi.org/10.1016/j.ijpharm.2019.118556.

[52] Khan Y, Durrani S, Siddique M, Mehmood M. Hydrothermal synthesis of alpha Fe2O3 nanoparticles capped by Tween-80. Materials Letters. 2011;65(14):2224-7. doi: https://doi.org/10.1016/j.matlet.2011.04.068.

[53] Monti D, Saccomani L, Chetoni P, Burgalassi S, Saettone M, Mailland F. In vitro transungual permeation of ciclopirox from a hydroxypropyl chitosan-based, water-soluble nail lacquer. Drug development and industrial pharmacy. 2005;31(1):11-7. doi: https://doi.org/10.1081/DDC-43935.

[54] Malhotra GG, Zatz JL. Investigation of nail permeation enhancement by chemical modification using water as a probe. Journal of pharmaceutical sciences. 2002;91(2):312-23. doi: https://doi.org/10.1002/jps.10058.

[55] Kobayashi Y, Miyamoto M, Sugibayashi K, Morimoto Y. Drug permeation through the three layers of the human nail plate. Journal of pharmacy and pharmacology. 1999;51(3):271-8. doi: https://doi.org/10.1211/0022357991772448.

[56] Bonesi CdM, Ulian LS, Balem P, Angeli VW. Carbamide peroxide gel stability under different temperature conditions: is manipulated formulation an option? Brazilian Journal of Pharmaceutical Sciences. 2011;47:719-24. doi: https://doi.org/10.1590/S1984-82502011000400008.

[57] Ismail SH, Hamdy A, Ismail TA, Mahboub HH, Mahmoud WH, Daoush WM. Synthesis and characterization of antibacterial carbopol/ZnO hybrid nanoparticles gel. Crystals. 2021;11(9):1092. doi: https://doi.org/10.3390/cryst11091092.

[58] Sharma K, Yadav V, Reang J, Sharma K, Tonk RK, Jain P, et al. Overview of the Current Advancements and Trends in the Transungual Drug Delivery System. Letters in Drug Design & Discovery. 2024;21(8):1316-24. doi: https://doi.org/10.2174/1570180820666230306140637.

[59] Szabó B, Süvegh K, Zelkó R. Effect of storage on microstructural changes of Carbopol polymers tracked by the combination of positron annihilation lifetime spectroscopy and FT-IR spectroscopy. International journal of pharmaceutics. 2011;416(1):160-3. doi: https://doi.org/10.1016/j.ijpharm.2011.06.028.

[60] Han Y, Qin X, Lin W, Wang C, Yin X, Wu J, et al. Microneedle-Based Approaches for Skin Disease Treatment. Nanomicro Lett. 2025;17(1):132. Epub 2025/02/06. doi: 10.1007/s40820-025-01662-y.

[61] Hameed HI, Al-Mayahy MH. Combined approach of nanoemulgel and microneedle pre-treatment as a topical anticellulite therapy. ADMET and DMPK. 2024;12(6):903-23. doi: https://doi.org/10.5599/admet.2461.

[62] Kim J-Y, Song J-Y, Lee E-J, Park S-K. Rheological properties and microstructures of Carbopol gel network system. Colloid and Polymer Science. 2003;281(7):614-23. doi: https://doi.org/10.1007/s00396-002-0808-7.

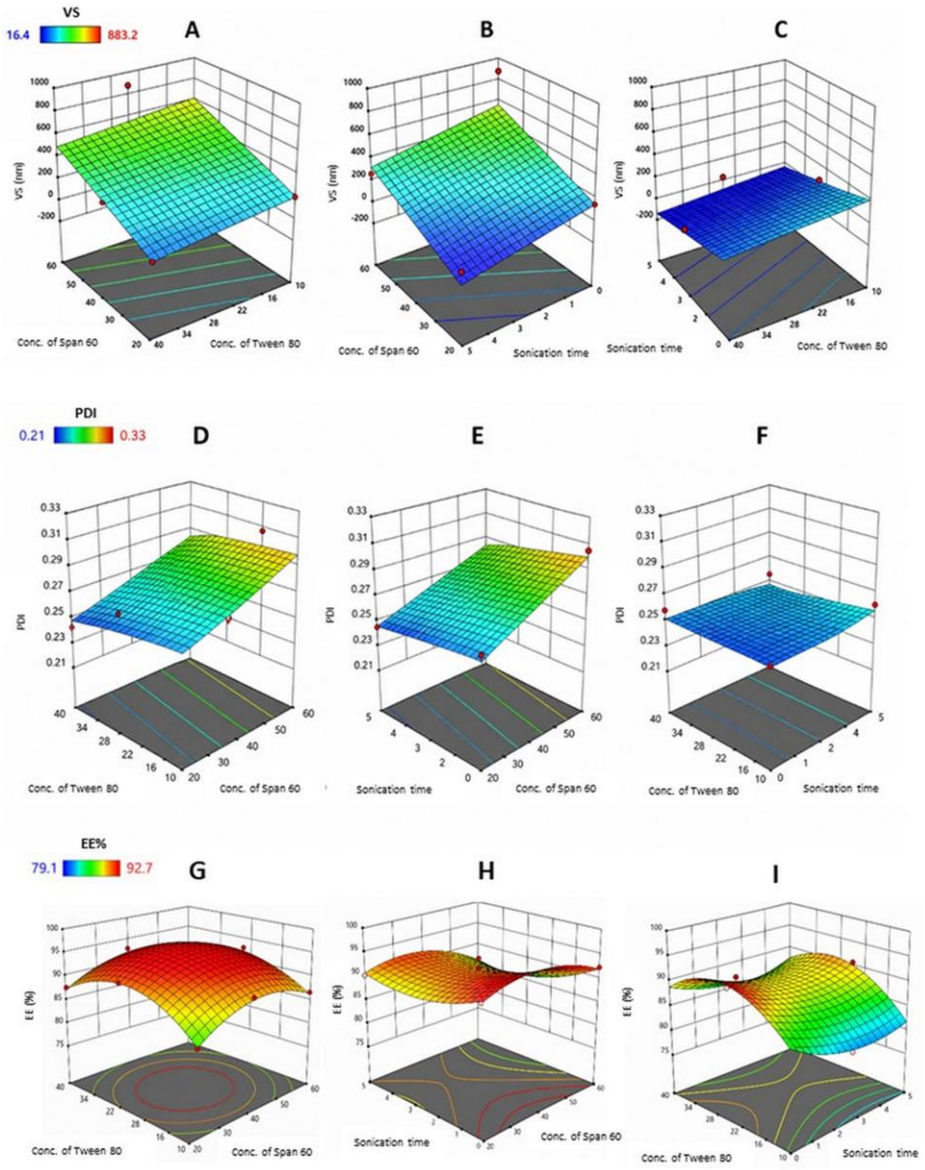

Figure 1. 3D surface plot representing the effect of independent variables (Conc. of Span 60, Conc. of Tween 80, and sonication time) on the VS, PDI, and EE%.

Natural Resources for Human Health
eISSN: 2583-1194

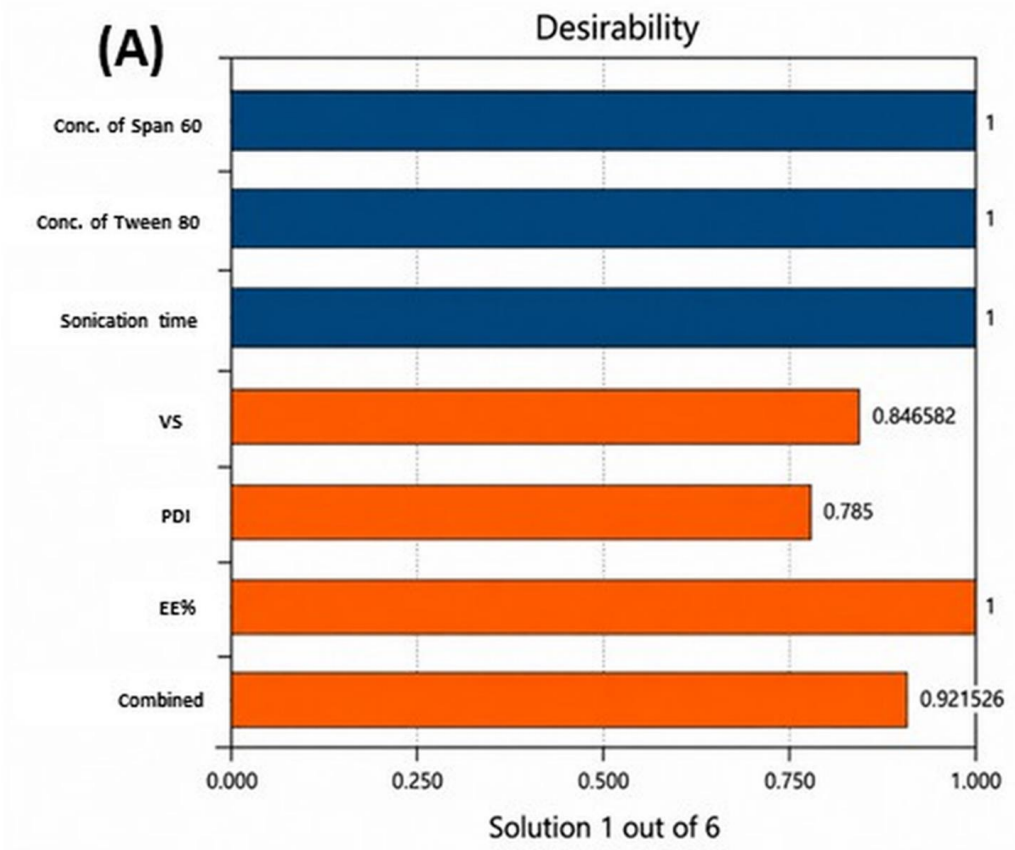

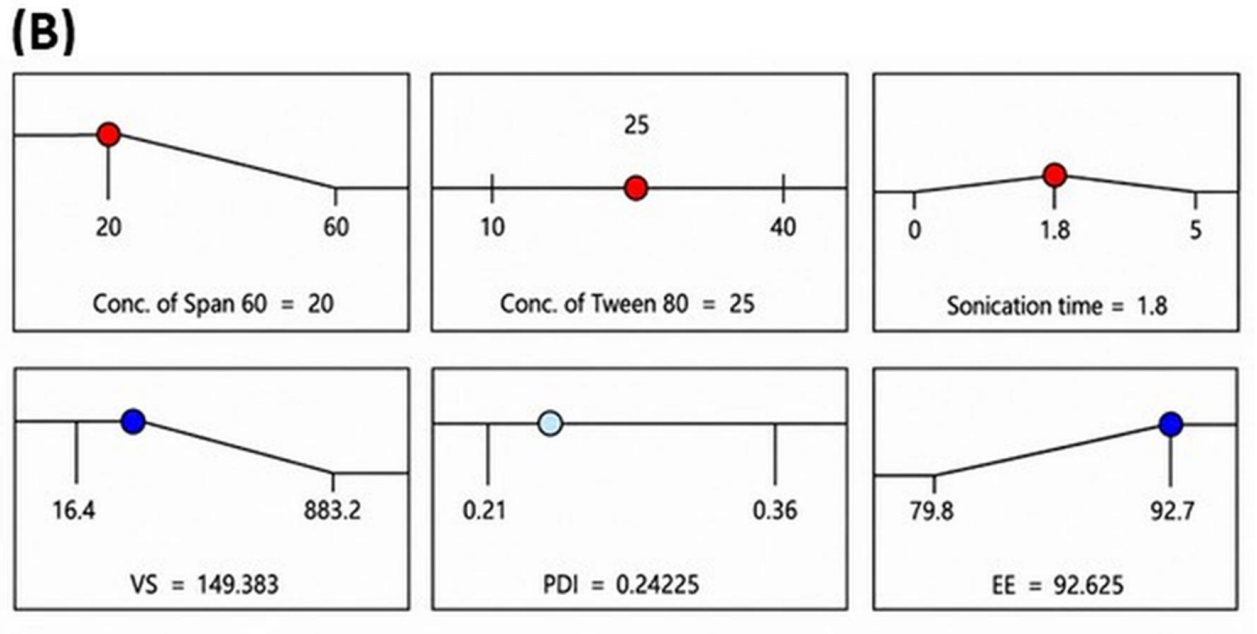

Figure 2. (A) The bar graph for the desirability of the optimisation process, (B) A graph for the optimised variable levels and predicted responses of the optimised CPO SP formulation.

Natural Resources for Human Health
eISSN: 2583-1194

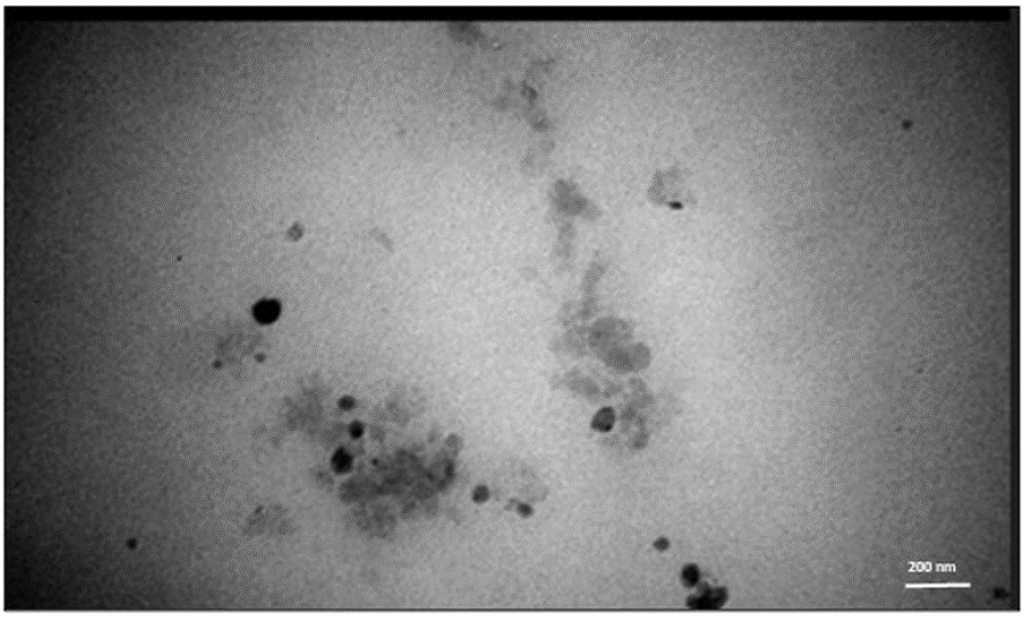

Figure 3. TEM image of the optimised SP formulation at a magnification of (50,000x).

Figure 4. Images of the inhibition zones of (A) SPs of CPO, (B) Solution of CPO in DMSO, and (C) Control solution.

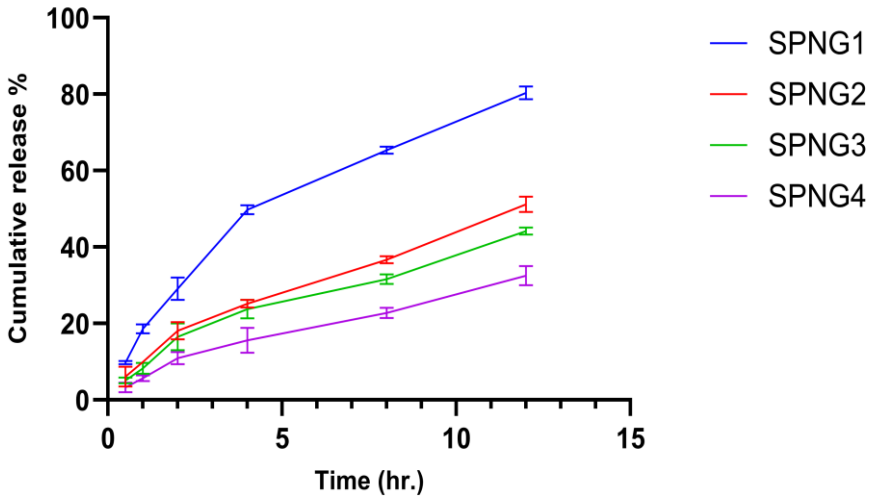

Figure 5. The accumulative release percentages of CPO SP nanogel formulations SPNG1, SPNG2, SPNG3, and SPNG4.

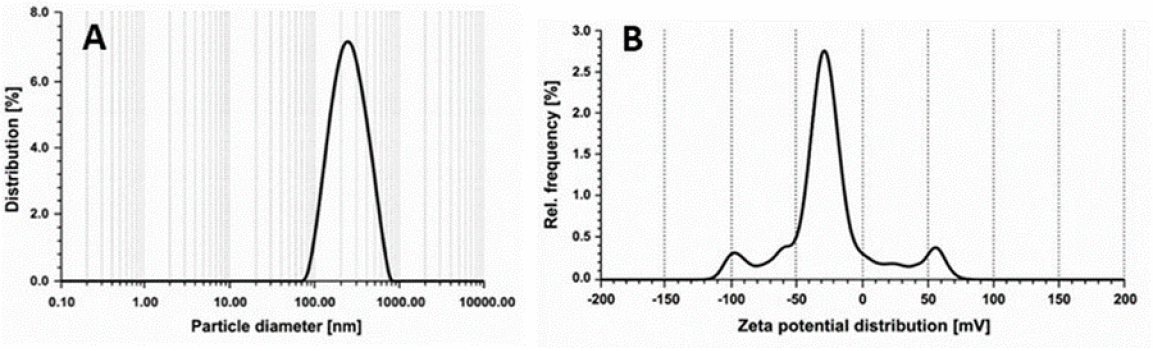

Figure 6. (A) Vesicle size distribution, and (B) Zeta potential distribution of the optimised SP nanogel formulation (SPNG1).

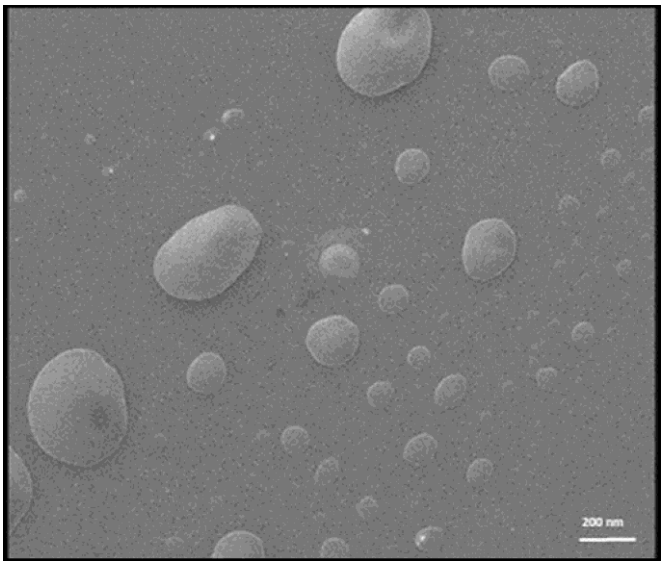

Figure 7. The Fe-SEM image of the optimised SP nanogel formulation (SPNG1).

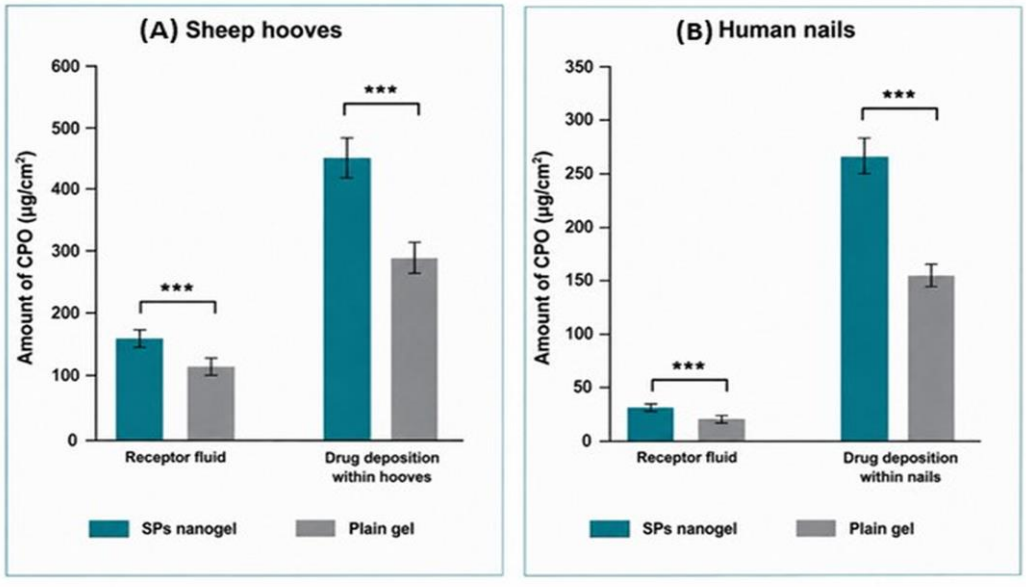

Figure 8. The amount of CPO (µg/cm²) from the SP nanogel and plain gel in receptor fluid and deposited amount in (A) Sheep hooves, and (B) Human nails. Data is presented as the mean ± SD (n = 6).

Natural Resources for Human Health
eISSN: 2583-1194

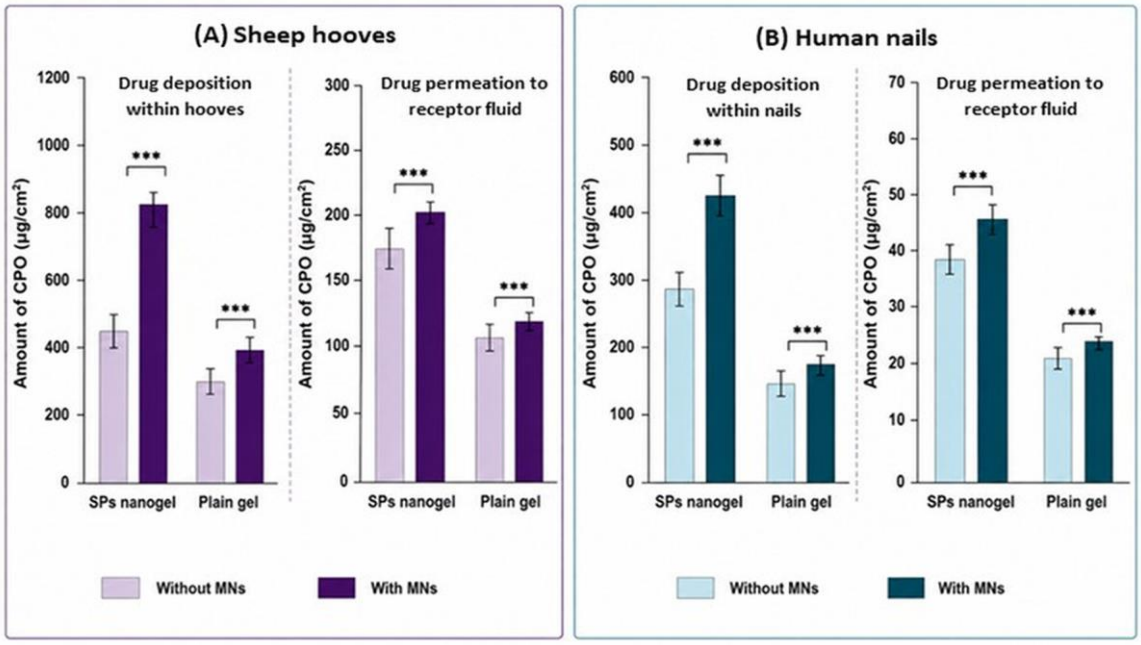

Figure 9. Effect of MNs on drug permeation and deposition from the SP nanogel and plain gel in (A) sheep hooves, and (B) human nails. Data is presented as the mean ± SD (n = 6).